DOI: 10.61782/fa.2023.0740

forum acusticum 2023

NUMERICAL CONDENSATION FOR HETEROGENEOUS POROUS MATERIALS AND METAMATERIALS

Abhilash Sreekumar[1,2*] **Fabien Chevillotte**[1] **Emmanuel Gourdon**[2]
[1] Matelys - Research Lab, 7 rue des Maraîchers, Bât. B, 69120 Vaulx-en-Velin, France
[2] Univ Lyon, ENTPE, Ecole Centrale de Lyon, CNRS, LTDS, UMR5513, 69518 Vaulx-en-Velin, France

ABSTRACT

Many acoustical porous materials are now heterogeneous. The heterogeneities arise due to recycling processes or are designed to add non-conventional phenomena (double porosity, multiple-scattering, Bragg interferences etc.). These materials are often called metamaterials.

Detailed Finite Element Models (FEM) of such materials prove prohibitively expensive, especially when embedded in large models like aircrafts. While heterogeneous analytical methods do exist only for specific or particular cases, a more robust generalization is derived by generating a condensed transfer matrix (TMM) from a single cell FEM computation. The coupled TMM-FEM approach is further improved by exploiting periodicity. This condensed- TMM is useful but dependent on the incident angle, that is, it must be recomputed for each incidence.

The present work couples the condensed-TMM with a numerical characterization of equivalent intrinsic parameters. These intrinsic parameters allow the heterogeneous material to be treated as a single layer in more complex structures and excitations like the diffuse field excitation.

The performance of the method, along with relevant examples will be discussed using an in-house code.

Keywords: *acoustical meta materials, material characterization, transfer matrix method, numerical condensation*

**Corresponding author*: *abhilash.sreekumar@entpe.fr.*

1. INTRODUCTION

Augmenting acoustical properties of sound barriers, especially absorption at low-frequencies, poses a research challenge to the Noise and Vibration Hardness community. State of the art solutions, such as multilayer systems or meta-materials are specifically developed to address these issues. Simulation techniques are necessary to achieve optimal design configurations for these solutions.

Contemporary methods such as the Finite Element Method (FEM) while robust, prove too expensive for detailed models and high-frequency applications. Analytical homogenization methods are used to take into account these heterogeneities [1] or non-conventional phenomena that are summarized in [2]. Nevertheless, the condensed TMM-FEM [3] harnesses the merits and drawbacks of both approaches to create a versatile and efficient technique to improve the accuracy of acoustical simulations of heterogeneous domains. However, the condensed TMM still needs to be recomputed for each angle of incidence - thereby proving expensive in diffuse field studies.

In this work, the authors use a numerical characterization approach, similar to an experimental technique [4], to estimate equivalent intrinsic parameters like dynamic mass density and bulk modulus from the condensed TMM for a single angle of incidence. These parameters are independent of the incident angle and are further exploited in simulating the acoustical response for other angles of incidence and diffuse field computations.

The paper is structured as follows: in Section 2, FE matrices are condensed to their TMM counterparts; followed by numerical extraction of intrinsic data. An example is considered in Section 3. Conclusions, limitations and future work are summarized in Section 4.

2. METHODOLOGY

A periodic structure comprising repeating cells is subjected to plane-wave excitation at oblique and azimuthal angles of incidence θ, α, respectively, in Fig. 1. The FE model for each unit cell as shown in Fig. 2 in the harmonic regime with excitation frequency ω is

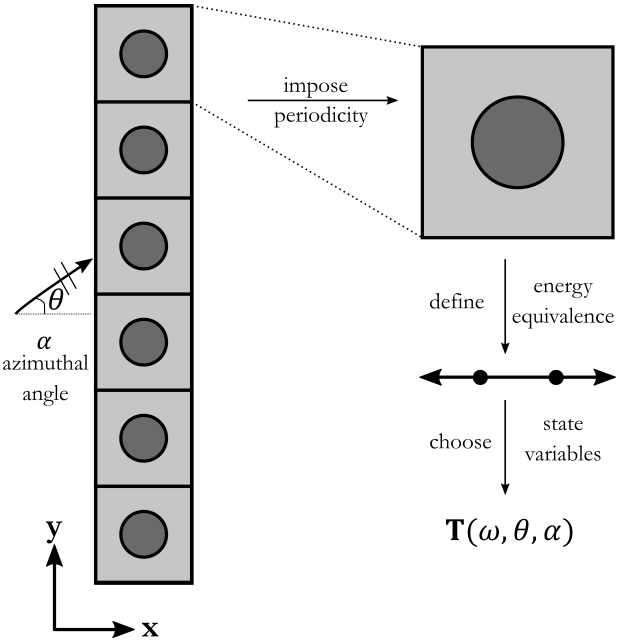

Figure 1: Procedural schematic for condensing FE matrices into TM matrices for a periodic heterogeneous structure.

$$\mathbf{D}(\omega)\mathbf{q} = \mathbf{b} \tag{1}$$

where matrix system is collected in the dynamic stiffness matrix $\mathbf{D}(\omega)$. The terms $\mathbf{q}$ and $\mathbf{b}$ represent the degrees of freedom and external load vector, respectively. This accommodates heterogeneous morphologies in the unit cell and admits solid and fluid interfaces.

Bloch's theorem is now applied to impose periodicity across the lateral boundaries

$$\mathbf{D}'(\omega, \theta, \alpha)\mathbf{q}' = \mathbf{b}', \tag{2}$$

where $\mathbf{D}'(\omega, \theta, \alpha)$, $\mathbf{q}'$ and $\mathbf{b}'$ are reduced-dimensional components of their original counterparts.

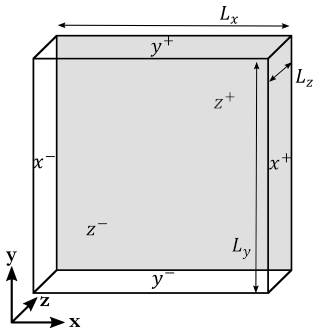

Figure 2: A periodic unit cell with labelling conventions. The wave-propagation occurs in $x-$ direction.

2.1 1-D energetic equivalence

Since the TMM is concerned with the states variables at the interfaces of the layers, the reduced DOF and external force vectors $\mathbf{q}'$ and $\mathbf{b}'$ are partitioned into incident (x^-), reception (x^+) and internal (I) dofs. Noting that $\mathbf{b}'_I = \mathbf{0}$, the internal DOFs $\mathbf{q}'_I$ are eliminated to yield the Schur-Complement condensation

$$\underbrace{\begin{bmatrix} \mathbf{D}'_{x^-x^-} - \mathbf{D}'_{x^-I}\mathbf{D}'^{-1}_{II}\mathbf{D}'_{Ix^-} & \mathbf{D}'_{x^-x^+} - \mathbf{D}'_{x^-I}\mathbf{D}'^{-1}_{II}\mathbf{D}'_{Ix^+} \\ \mathbf{D}'_{x^+x^-} - \mathbf{D}'_{x^+I}\mathbf{D}'^{-1}_{II}\mathbf{D}'_{Ix^-} & \mathbf{D}'_{x^+x^+} - \mathbf{D}'_{x^+I}\mathbf{D}'^{-1}_{II}\mathbf{D}'_{Ix^+} \end{bmatrix}}_{\mathbf{C}'} \begin{Bmatrix} \mathbf{q}'_{x^-} \\ \mathbf{q}'_{x^+} \end{Bmatrix} = \begin{Bmatrix} \mathbf{b}'_{x^-} \\ \mathbf{b}'_{x^+} \end{Bmatrix}. \tag{3}$$

where the DOFs on the incident face, $\mathbf{q}'_{x^-}$ are expressed in terms of the amplitude $\hat{\mathbf{q}}_{x^-}$

$$\mathbf{q}'_{x^-} = \mathbf{L}_{x^-}\hat{\mathbf{q}}_{x^-}, \tag{4}$$

where $\mathbf{L}_{x^-}$ collects the spatial distribution of the plane-waves $e^{-j(k_y y_{x_i^-} + k_z z_{x_i^-})}$ on the incident face. Using Eqs. (3)-(4) and rearranging, one obtains

$$\begin{Bmatrix} \hat{\mathbf{q}}_{x^-} \\ \hat{\mathbf{b}}_{x^-} \end{Bmatrix} = \mathbf{T}'(\omega, \theta, \alpha) \begin{Bmatrix} \hat{\mathbf{q}}_{x^+} \\ \hat{\mathbf{b}}_{x^+} \end{Bmatrix} \tag{5}$$

In the context of fluid and rigid-skeleton porous media, $\mathbf{T}'$ relates pressures and external forces. To obtain meaningful acoustical indicators, e.g., Sound Absorption Coefficient (SAC) and Sound Transmission Loss (STL), it is more convenient to work with pressures p and normal velocities v_x. Consequently, further manipulation of $\mathbf{T}'$ is necessary.

The requested state variable at an interface in such cases is

$$\mathbf{V} = [p, v_x]^T \tag{6}$$

where the normal velocity v_x is

$$v_x = \pm \frac{b}{j\omega\rho_f L_y L_z}, \tag{7}$$

with ρ_f denoting fluid density of external fluid and $j^2 = -1$. This relation between v_x and b is exploited to obtain the final transfer matrix

$$\begin{Bmatrix} \hat{\mathbf{p}}_{x-} \\ \hat{\mathbf{v}}_{x-} \end{Bmatrix} = \mathbf{T}(\omega, \theta, \alpha) \begin{Bmatrix} \hat{\mathbf{p}}_{x+} \\ \hat{\mathbf{v}}_{x+} \end{Bmatrix} \tag{8}$$

with

$$\mathbf{T}(\omega, \theta, \alpha) = \begin{bmatrix} 1 & 0 \\ 0 & 1/(j\omega\rho_f L_y L_z) \end{bmatrix} \mathbf{T}' \begin{bmatrix} 1 & 0 \\ 0 & -j\omega\rho_f L_y L_z \end{bmatrix} \tag{9}$$

Equivalent intrinsic parameters can now be obtained from $\mathbf{T}$ by comparing with the standard form [5]

$$\hat{\mathbf{T}}(\omega) = \begin{bmatrix} \cos(k_x(\omega)L_x) & j\omega\frac{\rho_{\text{eq}}(\omega)}{k_x(\omega)}\sin(k_x(\omega)L_x) \\ -\frac{k_x(\omega)}{j\omega\rho_{\text{eq}}(\omega)}\sin(k_x(\omega)L_x) & \cos(k_x(\omega)L_x) \end{bmatrix} \tag{10}$$

Assuming symmetry of the unit-cell and corresponding transfer matrix, one obtains the wave-number in propagation direction

$$k_x(\omega) = \frac{1}{L_x}\text{acos}(T_{11}), \tag{11}$$

where acos denotes the inverse-cosine operator and T_{ij} is the i^{th} row, j^{th} column entry in $\hat{\mathbf{T}}(\omega)$. The characteristic wave-number $k_{\text{eq}}(\omega)$ is computed

$$k_{\text{eq}}(\omega) = \sqrt{k_x^2 + k_y^2 + k_z^2}, \tag{12}$$

where the lateral wave-numbers k_y and k_z are already known

$$k_y = \frac{\omega}{c}\sin(\theta)\cos(\alpha), \; k_z = \frac{\omega}{c}\sin(\theta)\sin(\alpha). \tag{13}$$

Next, the equivalent mass density ρ_{eq} is evaluated

$$\rho_{\text{eq}}(\omega) = \frac{k_x}{\omega}\sqrt{\frac{T_{12}}{T_{21}}}. \tag{14}$$

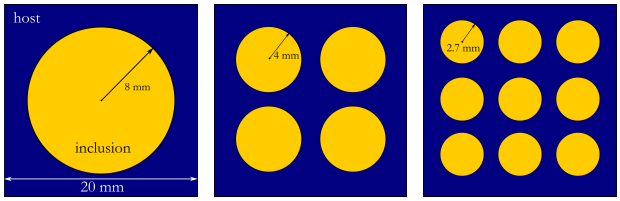

(a) A: unit cell with single inclusion (b) B: unit cell with array of 2×2 inclusions (c) C: unit cell with array of 3×3 inclusions

Figure 3: Three unit cell configurations considered for numerical characterization.

The equivalent bulk modulus $K_{\text{eq}}(\omega)$ can be obtained from ($k_{\text{eq}}(\omega)$, $\rho_{\text{eq}}(\omega)$) with the relation

$$k_{\text{eq}}(\omega) = \omega\sqrt{\frac{\rho_{\text{eq}}(\omega)}{K_{\text{eq}}(\omega)}}. \tag{15}$$

The characteristic impedance $Z_{\text{eq}}(\omega)$ can also be evaluated:

$$Z_{\text{eq}}(\omega) = \sqrt{\rho_{\text{eq}}(\omega)K_{\text{eq}}(\omega)}. \tag{16}$$

This permits near instantaneous computations of SAC and STL for plane-waves at other angles of incidence and diffuse field excitations. This numerical characterisation approach stands in stark contrast to classical FE and TMM techniques where stiffness and transfer matrices are freshly re-evaluated for each angle of incidence with Eqs. (10) and (13).

3. RESULTS AND DISCUSSION

A 20×20 mm unit cell repeating periodically in the y and z directions is considered. Three configurations A, B and C, with 1, 4 and 9 rigid-skeleton porous inclusions, respectively, embedded within a rigid-porous host material are studied, as shown in Fig. 3.

The size of all inclusions are determined such that the total inclusion volume-fraction is 0.5. The influence of the degree of heterogeneity on the method is quantified by varying the resistivity contrast between the host and inclusion materials. The macroscopic parameters used are summarized in Table 1.

Configurations A, B and C are numerically characterized at incident angle $\theta_{\text{carac}} = 45°$ with varying resistivity contrasts as described in Table 1. The intrinsic parameters ρ_{eq} and K_{eq} obtained from this procedure are then used

Table 1: JCA Macroscopic parameters for the host and inclusion rigid-skeleton porous materials.

	Host	**Inclusion**		
		I	**II**	**III**
σ $[N \cdot m \cdot s^{-4}]$	8900	2×10^4	2×10^6	2×10^7
ϕ		0.95		
α_∞	1.42		1	
$\lambda\ [m]$	100×10^{-6}	8.802×10^{-6}	8.802×10^{-6}	2.783×10^{-6}
$\lambda'\ [m]$	360×10^{-6}			

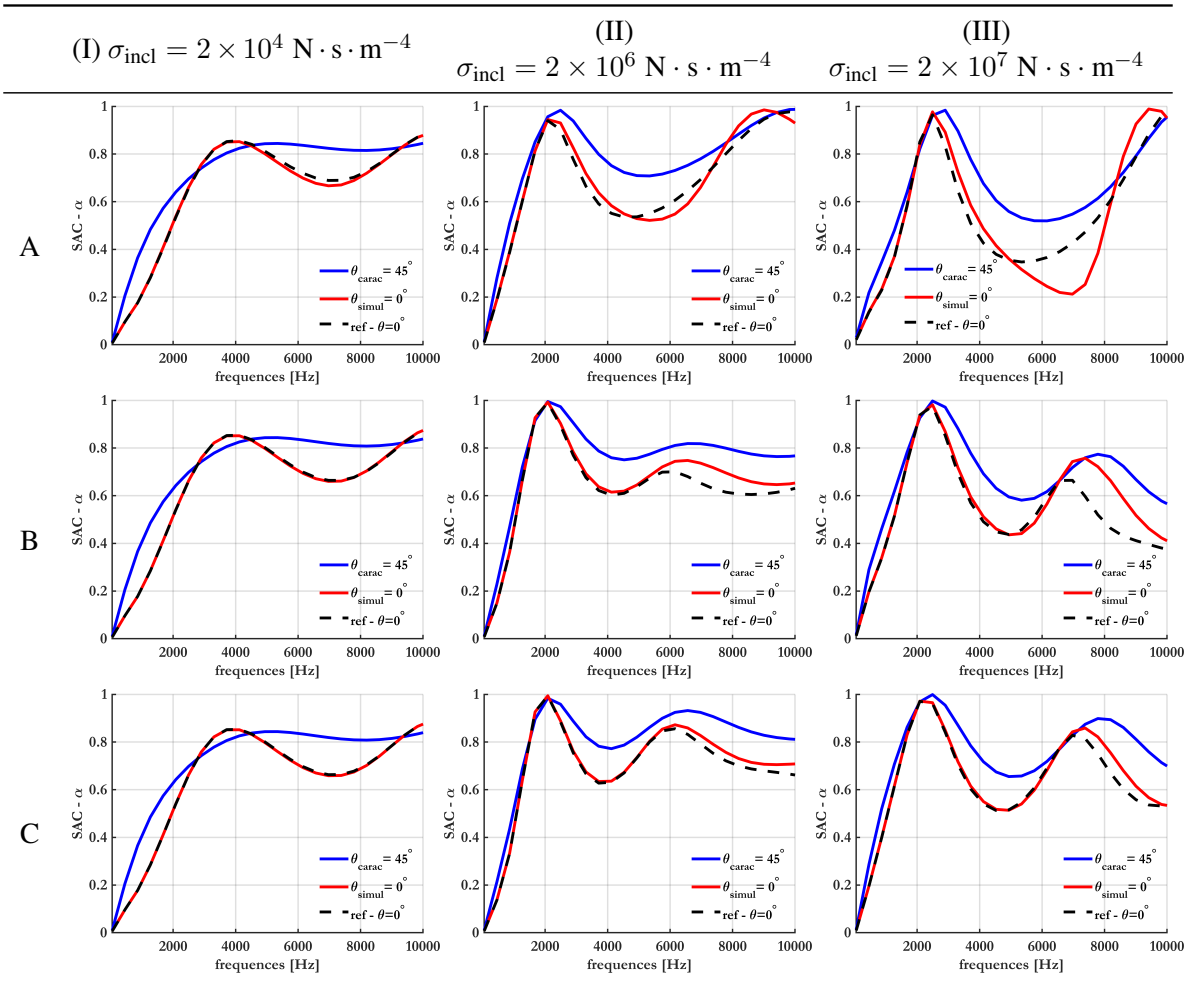

Table 2: SAC obtained for plane-wave excitation at normal incidence $\theta_{\text{simul}} = 0°$ by intrinsic parameters characterized from $\theta_{\text{carac}} = 45°$.

to simulate the SAC for a frequency range of [20 Hz, 10 kHz] at normal incidence, i.e., $\theta_{\text{simul}} = 0°$. The results are illustrated in Table 2.

In Table 2, the simulated curves in red at $0°$ exactly coincide with the reference FE results in black for the case with low resistivity contrast $\sigma_{\text{incl}} = 2\times10^4$ N·s·m^{-4}, i.e., A(I), B(I), C(I). The accuracy diminished with increase in heterogeneity, e.g., in A(III), significant discrepancies between the simulated and reference curves are observed in between 5 and 8 kHz. The extremely high inclusion resistivity is chosen to mimic an infinite rigid inclusion and thereby demonstrate the limits of the characterization approach.

Further, a decreasing trend in characterization accuracy is observed with increasing inclusion size with the same total volume fraction and resistivity, as seen in A(III), B(III) and C(III), respectively, especially at high frequencies. This is attributed to the ratio between high frequency wavelengths and size of the inclusions under consideration.

Table 2 is purely illustrative in nature and does not offer anything significant by way of computational efficiency. The primary interest in the TMM-FEM based numerical characterization lies in its ability to drastically reduce computational run-times for diffuse field excitations with compromising simulation accuracy. Using the same characterized parameters in Table 2, i.e., for $\theta_{\text{carac}} = 45°$, the SAC obtained for such diffuse field excitation are provided in Table 3.

The differences between the reference and simulated curves in the high permeability (III) for all three configurations is much smaller in comparison to the single incident angle simulation in Table 2. This demonstrates the method to be effective tool for diffuse field simulations, even in highly heterogeneous unit cell configurations. The associated computational run times of the numerical characterization approach and its speed up relative to the full FE simulation for diffuse field runs is provided in Table 4.

All run-times are averaged over three runs. The diffuse field SAC is obtained by integrating over 32 angles of incidence varying from $0°$ to $90°$. The total run-time of the numerical characterization procedure accounts for the FEM-TMM condensation and characterization procedure for a single angle of incidence; and subsequent runs over the 32 incident angles using the obtained intrinsic parameters. An appreciable speed-up of 36.7 over the full FE approach is exhibited by our method.

4. CONCLUSIONS AND FUTURE STAKES

The TMM-FEM was used in this work to numerically characterize heterogeneous periodic materials. The resulting intrinsic parameters are used to formulate a transfer matrix that is angle-of-incidence independent, thereby greatly accelerating diffuse field simulations. The accuracy and efficiency of the method pertaining to heterogeneous inclusions is successfully demonstrated. The accuracy is strongly dependent on the incident-angle chosen for characterization, the degree of heterogeneity in the unit cell and frequency bandwidth desired.

This condensation technique has two advantages. The first one is to speedup the computation, especially when considering large systems like aircrafts or automotives including heterogeneous materials or meta-materials. The second one is to analyze the intrinsic parameters to understand the overall effect of such heterogeneity or non-conventional phenomena.

The example considered in this work is restricted to fluids and symmetric configurations only. However, the method is applicable to elastic and poro-elastic media as well. Accommodating asymmetry through a third intrinsic parameter, i.e., the coupling term χ [6] is a second generalisation of the approach. Finally, incorporating higher-order Bloch modes [7] to improve characterization and simulation results at high frequencies is another proposed improvement to the method.

5. ACKNOWLEDGMENTS

The authors acknowledge the support of the French Agence Nationale de la Recherche (ANR) under project (PROJET FRANCE-RELANCE DE PRESERVATION DE L'EMPLOI R&D). The work has been conducted in the framework of CeLyA (Lyon Acoustics Center, ANR-10-LABX-0060). A. Sreekumar is grateful to Dr. François-Xavier Bécot, Dr. Fabien Marchetti and Prof. Olivier Dazel for fruitful discussions on numerical characterization and TMM condensation.

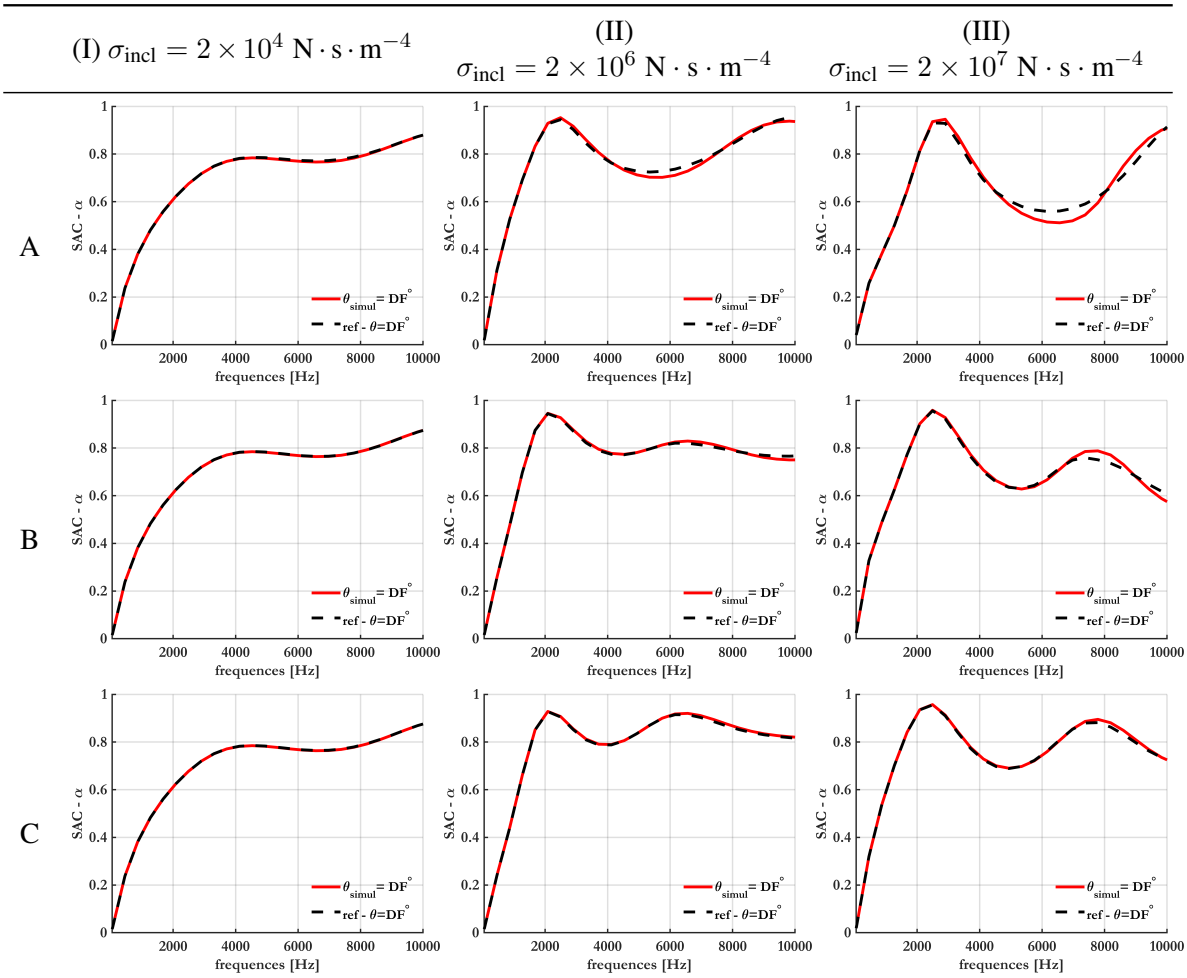

Table 3: SAC obtained by intrinsic parameters characterized from $\theta_{\text{carac}} = 45°$; for diffuse-field excitation.

Table 4: Run-times for full FEM and FEM-TMM approach with numerical characterization for diffused-field excitation with 32 incident angles.

	Time
Full FEM	125 s
FEM-TMM	3.4 s

6. REFERENCES

[1] F. Chevillotte, F.-X. Bécot, and L. Jaouen, "On the modeling of visco-thermal dissipations in heterogeneous porous media," *J. Acoust. Soc. Am*, vol. 138, no. 6, pp. 3922 – 3929, 2015.

[2] F. Chevillotte, F.-X. Bécot, and L. Jaouen, "Classification of non-conventional phenomena involved in meta-materials,"

[3] A. Parrinello and G. Ghiringhelli, "Transfer matrix representation for periodic planar media," *Journal of Sound and Vibration*, vol. 371, pp. 196–209, 2016.

[4] Y. Salissou and R. Panneton, "Wideband characterization of the complex wave number and characteristic impedance of sound absorbers," *The Journal of the Acoustical Society of America*, vol. 128, no. 5, pp. 2868–2876, 2010.

[5] J.-F. Allard and G. Daigle, "Propagation of sound in porous media: Modeling sound absorbing materials," 1994.

[6] J.-P. Groby, M. Malléjac, A. Merkel, V. Romero-García, V. Tournat, D. Torrent, and J. Li, "Analytical modeling of one-dimensional resonant asymmetric and reciprocal acoustic structures as willis materials," *New Journal of Physics*, vol. 23, no. 5, p. 053020, 2021.

[7] A. Parrinello, G. Ghiringhelli, and N. Atalla, "Generalized transfer matrix method for periodic planar media," *Journal of Sound and Vibration*, vol. 464, p. 114993, 2020.